3956

UPWELLING VARIABILITY AT JARVIS ISLAND

A THESIS SUBMITTED TO THE GRADUATE DIVISION OF THE
UNIVERSITY OF HAWAI'I IN PARTIAL FULFILLMENT
OF THE REQUIREMENTS FOR THE DEGREE OF

MASTER OF SCIENCE

IN

OCEANOGRAPHY

MAY 2005

By
Jamison M. Gove

Thesis Committee:

Mark Merrifield, Chairperson
Russell Brainard
Eric Firing
Robert Bidigare

DEDICATION

I dedicate this thesis to my grandmother, Catherine Tice. Thank you for your eternal support and encouragement and for playing such a significant and influential role throughout my life. You have and always will be an inspiration to us all.

ACKNOWLEDGEMENTS

I would like to express the utmost gratitude to Dr. Mark Merrifield for the tremendous amount of time, supervision, and assistance he gave me throughout this research. His guidance and advice will stay with me for many years to come. I would like to thank Dr. Russell Brainard not only for funding this research, but for initially presenting me with the opportunity to work on such a fascinating and exciting project. I am also thankful to Dr. Eric Firing and Dr. Robert Bidigare for their valuable comments and help during this project.

I would like to thank the many individuals who contributed greatly to this research including Yvonne Firing, Jules Hummond, Ronald Hoeke, Robert Schroeder, Matthew Dunlap, Oliver Dameron, Molly Timmers, Shikiko Nakahara, Dave Foley, Jerome Aucan, June Firing, and a number of additional SOEST, CRED, and PIFSC staff.

Special thanks to Nancy Koike for the significant help with the seemingly endless amount of forms and paperwork associated with graduate school and to both Nancy and Rene Tada for always having such a positive influence on my day.

I am especially thankful and indebted to my family who has given me a substantial amount of support and love. Particularly I would like to thank my mother, sister, and grandmother for being such a solid foundation throughout my life and for their invaluable advice and constant encouragement.

Lastly, I would like to thank my friends, who have played a crucial role in my happiness throughout this research and my life here in Hawai'i.

ABSTRACT

The interaction of the equatorial undercurrent (EUC) with Jarvis Island results in localized upwelling on the western (upstream) side of the island. Observed fish densities and benthic habitat distributions relate strongly to the upwelling pattern. A simple diagnostic model based on the Bernoulli equation confirms that upwelling depends on the depth of the thermocline and the strength and depth of the EUC, which are modulated by equatorial wind forcing. Strongest upwelling at Jarvis occurs in boreal spring when annual wind forcing leads to a shallow thermocline and shallow and strong EUC. Interannual variations in seasonal upwelling are tied to ENSO; La Niña conditions enhance upwelling at Jarvis by inducing a regional shoaling of the thermocline and the EUC. On intraannual time scales, cessation or reversal of strong westerly wind events in the western Pacific generates Kelvin waves, which are upwelling-favorable at Jarvis. Trade wind relaxations in the central Pacific result in strong eastward surface jets at Jarvis (> 1.00 m s^{-1}); however, these events are downwelling favorable. During periods of EUC-driven upwelling, interactions of the semidiurnal tide with Jarvis result in abrupt cold spikes (1-4°C) that tend to occur at ~12 hour periods. Tidal currents and temperature fluctuate 180° out of phase, such that maximum upwelling coincides with maximum eastward current. The presence of internal tides, either locally or remotely generated, likely accounts for the tidal upwelling signal.

TABLE OF CONTENTS

LIST OF FIGURES

CHAPTER 1: INTRODUCTION

Jarvis Island is a small island (~4.5 km^2) located in the central equatorial Pacific at 0° 22.5'S, 160° 1.0'W (Figures 3.1, 3.2). Its proximity to the equator and isolation from neighboring islands causes Jarvis to be directly in the path of the high velocity equatorial undercurrent (EUC). The interaction of the EUC with Jarvis has been the focus of previous studies (Hendry and Wunsch, 1973; Roemmich, 1984; henceforth HW73 & R84, respectively). HW73 observed isotherm uplift on the west (upstream relative to the EUC) side of Jarvis compared to the east. They attributed this to the blocking of the EUC by Jarvis, resulting in flow stagnation and positive vertical isotherm displacements on the upstream side in accord with the Bernoulli equation for steady, inviscid flow past a cylindrical island. R84 found island pressure measurements to be consistent with this scenario.

Oceanographic settings are inherently variable, especially when considering an isolated island in the equatorial Pacific. Although variability in Bernoulli driven upwelling was not a point of discussion in either of the previous studies, we observe that isopycnal displacements and near shore temperatures vary on interannual to semidiurnal time scales. We find that upwelling variability at Jarvis depends on a variety of large-scale, low frequency processes including the El Niño-Southern Oscillation (ENSO), intraseasonal equatorial trapped Kelvin waves, surface jets associated with trade wind relaxations, and seasonal variations in the strength and depth of the EUC. In addition, when conditions are conducive for EUC-driven upwelling, interactions of the semidiurnal tide with the island result in high frequency temperature changes at the surface.

Like most near-equatorial islands, Jarvis features a well-developed coral reef ecosystem (Maragos, 2004). Variable intrusions of cold water to the surface layer can potentially serve as an important source of nutrients and suspended particles (Leichter and Miller, 1999), thereby enhancing overall reef ecosystem productivity. We find that the spatial variation in benthic habitat and planktivore distributions are strongly influenced by upwelling at Jarvis. Both show a marked correspondence with the spatial upwelling pattern.

In an attempt to assess upwelling variability near Jarvis, this paper incorporates data from previous studies: oceanographic and biological data from three recent Coral Reef Ecosystem Division (CRED) ship surveys of Jarvis; various meteorological and oceanographic data from the Tropical Atmosphere Ocean (TAO) array; satellite derived zonal surface currents and SST; historical sea level data obtained from the University of Hawaii Sea Level Center (UHSLC); and a two-year time series of *in-situ* data from a current-temperature-salinity mooring. The objectives of this research are to describe the large-scale oceanographic variability in the vicinity of Jarvis Island that promotes EUC-driven upwelling, to assess the role of equatorial Pacific winds in establishing these conditions, and to consider tidal enhancement of EUC-driven upwelling on semidiurnal time scales.

The paper is organized as follows: previous studies at Jarvis and the general oceanographic conditions in the region are summarized (Section 2); the datasets used in this paper are described (Section 3); recent hydrographic and ecological surveys are used to depict spatial patterns of upwelling and biological conditions at Jarvis (Section4); moored data at Jarvis and at nearby TAO buoys are used to describe temporal variations

in upwelling (Section 5); the importance of western Pacific winds and associated basin-wide adjustments to upwelling/downwelling Kelvin waves is considered (Section 6); observed upwelling at Jarvis is shown to be consistent with a model for EUC-driven upwelling based on the Bernoulli equation (Section 7); cold temperature spikes at the semidiurnal period are considered in relation to tidal processes (Section 8); and the major results are summarized and suggestions for future work are considered (Section 9).

CHAPTER 2: BACKGROUND

2.1 Previous Studies of Jarvis Island

Through a series of salinity-temperature-depth (STD) casts taken during a two-day survey of Jarvis in April 1971, HW73 noted large deflections and vertical spreading of isopycnals directly upstream (west) and a distinct wake effect downstream (east) of the island. Upstream isopycnal deflections were found to be consistent with the Bernoulli equation (1) describing inviscid, steady, stratified shear flow past an obstacle;

$$\frac{1}{2}u^2 + g\zeta - D \equiv B \qquad (1)$$

where u is the horizontal velocity in the x-direction, g is gravity, ζ is the sea surface elevation and D is the "dynamic depth" ($m^2\ s^{-2}$) defined by;

$$D = \int_{P_{atm}}^{p} \alpha(x, y, p')dp' \qquad (2)$$

where α is the specific volume of water in $cm^2\ g^{-1}$, p is the pressure level in decibars, x and y are horizontal coordinates and P_{atm} is the atmospheric pressure at the sea surface. The Bernoulli constant (B) is conserved following streamlines, hence reduction in flow near Jarvis results in pressure increases associated with ζ and/or D. HW73 assumed a negligible ζ contribution compared to the baroclinic term. Thus, isotherm displacements are related directly to changes in flow speed.

Using the ideal fluid model of Drazin (1961) and the potential flow solution of Lamb (1932), HW73 computed isopycnal displacements (z) from a rest state (z_o) caused by flow around a cylindrical island as

$$z - z_o = J^{-1}M(q_1^{\ 2} - 1) + O(J^{-2}) \qquad (3)$$

where $$J = N^2/(V/h)^2 \text{ and } M = U\frac{dU}{dz_o}\Big/(V^2/h) \qquad (4)$$

Far upstream, positive zonal flow $U(z)$ and density $\rho(z)$ are specified, V is the velocity scale, h is the height scale, $N^2 = (-g/\rho)\frac{d\rho}{dz_o}$ is the square of the Brunt-Väisälä frequency, $(q_1^{\,2} - 1)$ is the velocity perturbation induced by an elliptical obstacle divided by the far field velocity as computed by Lamb (1932), and both J and M are non-dimensional. When applied outside the downstream wake region, HW73 found that the scale of displacement of a particular density surface computed by

$$UN^{-2}(dU/dz_o) \qquad (5)$$

is in good agreement with observed isopycnal displacements.

Expanding on the findings of HW73, R84 conducted two ship surveys in November 1982 and March 1983 around Jarvis to study the energetics of a swift current encountering an island obstacle. Using an array of temperature-pressure recorders, temporal variations in the pressure field around Jarvis were estimated and used to compute the free stream velocity. Rather than assuming negligible surface effects, R84 observed current velocity close to zero at 250 m and assumed the pressure field was approximately uniform at this particular depth, thus allowing for the vertical integration of the hydrostatic relation to obtain the pressure distribution around the island. R84 showed that potential energy increases and kinetic energy decreases as the flow approaches the upstream stagnation point and computed the pressure elevation to be $\sim\frac{1}{2}u^2$ at the stagnation point, in accord with the analytic results of HW73.

Wyrtki and Eldin (1982) examined locally wind-driven upwelling in the Jarvis Island region, which is distinct from upwelling caused by flow interaction with the island.

During an 18 month study from February 1979 to June 1980, Wyrtki and Eldin used equatorial cross-sections from the Hawaii-Tahiti Shuttle Experiment, zonal wind speeds measured at Jarvis and at a mooring near 153°W, and SST and sea level from Jarvis to capture equatorial upwelling events (defined as a positive vertical migration of the 26°C isotherm). Five distinct easterly wind bursts (6-10 m s^{-1}), each lasting ten days to three weeks, caused a decrease in sea level and SST at Jarvis, and an average vertical migration of 3-5 m day^{-1} of the 26°C isotherm near 153°W. Wyrtki and Eldin concluded that easterly winds result in Ekman transport away from the equator, a decrease in sea level, an uplift of isotherms, and an eventual decrease in SST.

2.2 Oceanographic Setting

The structure of the Pacific equatorial current system, specifically the EUC, has been well studied by numerous investigators (Cromwell, 1953; Knauss, 1960; Wyrtki et al., 1981; Firing, 1981; Firing et al., 1983; Wyrtki and Kilonsky, 1984; Yu and McPhaden, 1999; Keenlyside and Kleeman, 2002). In general, the equatorial region is dominated by easterly trade winds spanning the Pacific basin. These winds force a complex system of westward-flowing surface currents and eastward-flowing surface and subsurface counter-currents. The EUC, a cold and nutrient rich (Chavez et al., 1999) eastward-flowing subsurface counter-current, lies along the equator and within the thermocline, with undercurrent core depths ranging from 200 m in the western Pacific to 20 m in the east, and a mean flow of 100 m s^{-1} (Yu and McPhaden, 1999). The South Equatorial Current (SEC), a westward-flowing current, lies directly above the EUC and is generally a much weaker and warmer current than the EUC (Yu and McPhaden, 1999; Keenlyside and Kleeman, 2002).

The equatorial Pacific has been an area of intense study primarily due to ENSO, which has a significant impact on regional and global climate (Yu and McPhaden, 1999). This variability strongly influences oceanographic and atmospheric conditions throughout the Pacific basin including sea surface temperature, precipitation, winds, currents, and biological production (Philander, 1990; McPhaden et al., 1998). During an El Niño, trade winds weaken and occasionally reverse in the equatorial Pacific, resulting in anomalously warm sea surface temperatures and eastward surface transport (Yu and McPhaden, 1999). These wind anomalies are typically in the form of westerly wind bursts in the western Pacific, which generate equatorial trapped Kelvin waves that propagate eastward, altering the sea surface slope and depressing the thermocline. During an El Niño, the EUC has been observed to weaken and, on rare occasions, reverse direction (Firing et al., 1983; Roemmich, 1984).

Oceanographic conditions in the equatorial Pacific display a prominent seasonal cycle. The EUC and upper thermocline undergo large seasonal vertical migrations in the central Pacific beginning in January, with maximum shoaling occurring during boreal springtime (Yu and McPhaden, 1999; Keenlyside and Kleeman, 2002). Sea surface heights seasonally vary 180° out of phase with thermocline depth, with minima (maxima) surface heights corresponding roughly to periods of shallowest (deepest) thermocline depth (Wyrtki and Eldin, 1982; Yu and McPhaden, 1999). Eastward zonal subsurface currents are strongest in boreal spring as a result of trade wind relaxations in the eastern Pacific, which cause a basin-wide adjustment of the pressure gradient (McPhaden et al., 1998). From the surface to the EUC core, a pronounced basin wide eastward surge occurs around April-July causing the EUC to strengthen and shoal, and the SEC to

weaken (McPhaden et al, 1998; Yu and McPhaden, 1999; Keenlyside and Kleeman, 2002). Conditions during boreal spring are the most conducive for EUC-driven upwelling at Jarvis.

CHAPTER 3: DATA COLLECTION

The Coral Reef Ecosystem Division (CRED), part of the Pacific Islands Fisheries Science Center, conducted a series of hydrographic and biological surveys around Jarvis Island during the winters of 2000-2002 on the R/V *Townsend Cromwell*. Hydrographic data include numerous shallow water CTD casts (max 30 m depth), shipboard Acoustic Doppler Current Profiler (SADCP) surveys, and SST measurements around the perimeter of Jarvis. Shallow water CTD casts were performed using a 2 Hz Sea Bird Electronics (SBE) 19 SEACAT profiler (accuracy of 0.001 ms cm^{-1} in conductivity, 0.01°C in temperature, and 0.25% in depth). The CTD profilers were hand-lowered off a small boat at approximately a 0.5 to 0.75 m s^{-1} descent rate to a maximum depth of 30 meters. During 2002, mechanical failures limited the spatial extent of the surveys. Specific locations of each cast were recorded using a hand held global positioning system (GPS). SST data were obtained from the shipboard SBE thermo-salinograph. SADCP measurements were taken using a 150 kHz narrow-band RDI ADCP. The system configuration was an 8 m pulse length, 8 m depth bins (re-gridded to 10 m depth bins) starting at 20 m and extending typically to 350 m, and 15 min averaged ensembles. SADCP data were not obtained on the east side of the island in 2000.

Biological data include fish surveys and towed diver benthic video surveys. Non-invasive underwater belt-transects were conducted to enumerate planktivore assemblages at replicate sites around Jarvis. During transects, a pair of scuba diver-observers conducted parallel swims along three 25 m long transect lines (10-15 m depth, 2 m width), recording fish number and length, enabling biomass density calculations by site (for further explanation see Schroeder et al., 2004). Benthic habitats were surveyed in

2002 using a towed diver on a towboard equipped with a downward high resolution digital video camera to quantify habitat composition and complexity. Further detail on belt-transect protocols, towboard protocols, and digital video data analysis is found in Kenyon et al. (2004).

A 22 month time series (March 2002 – December 2003) of temperature and current measurements was obtained from a 3 beam configured 1000 kHz SonTek Acoustic Doppler Profiler (ADP) with an attached SBE 37 MicroCAT temperature-salinity recorder moored on the bottom in 14 m of water off the southwest tip of Jarvis (Figure 3.1). SBE 37 temperature and salinity data were sampled every 15 min. Current and temperature from the ADP were averaged for 7 min every 2 hr through the deployment.

Equatorial Pacific oceanographic conditions were specified using the Tropical Atmosphere-Ocean (TAO) array buoy data, including zonal wind, subsurface temperature and 20°C isotherm depth anomalies. Zonal ADCP currents and the depth of the 25°C isotherm were obtained from two specific TAO buoys on the equator at 170°W and 155°W, 1000 km and 500 km away from Jarvis, respectively (Figure 3.2). Satellite derived zonal ocean currents were obtained from the National Oceanic and Atmospheric Administration's (NOAA) Ocean Surface Current Analysis – Real time (OCSCAR) model and Pathfinder 9 km resolution SST data were obtained from the Central Pacific Node of NOAA Coast Watch.

Sea level data were obtained from the Christmas Island (1° 59.0'N, 157° 28.0'W) tide gauge maintained by the UHSLC (Figure 3.2). Sea level was also measured on Jarvis Island from September 1981 to December 1987. Although tide gauge

observations at Jarvis were not available during the time of the CRED surveys, the Jarvis record is well correlated with that of Christmas Island (correlation of 0.91). Thus, we use Christmas Island tide gauge data as a proxy to represent sea level variations at Jarvis.

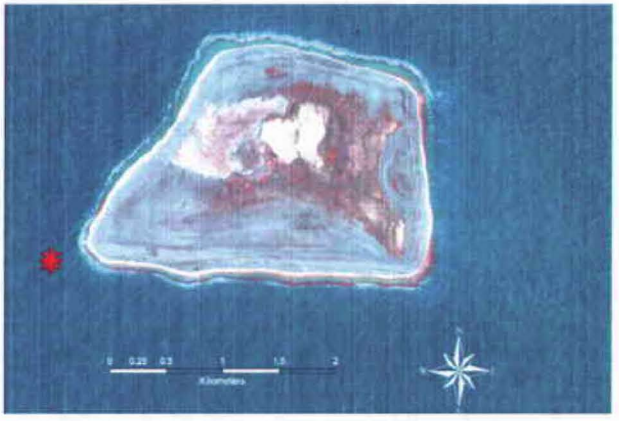

Figure 3.1 An Ikonos satellite image of Jarvis Island showing the location of the Acoustic Doppler Profiler (ADP) and SBE 37 MicroCAT temperature-salinity recorder moored on the bottom in 14 m water depth.

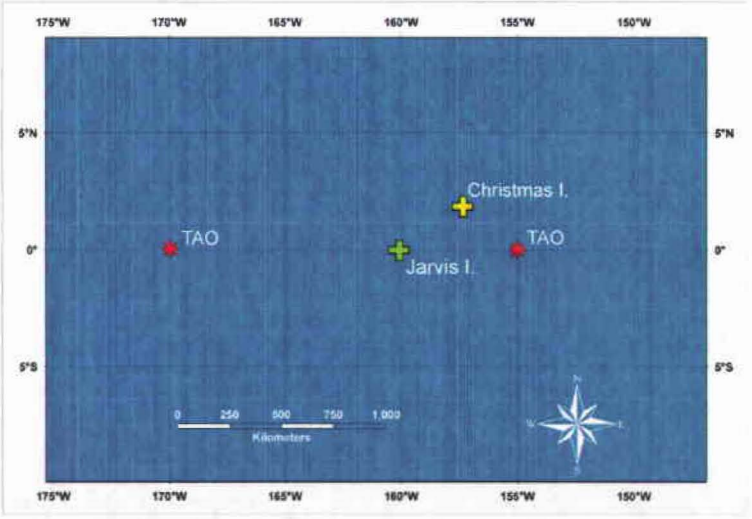

Figure 3.2. Sea level data are obtained from Christmas Island (01° 59.0'N, 157° 28.0'W) and zonal ADCP data and depth of the 25°C isotherm are obtained from TAO buoys at 0°, 170°W and 0°, 155°W, respectively.

CHAPTER 4: SPATIAL SURVEYS OF ISLAND UPWELLING

4.1 Current Structure

The SADCP data indicate the strength and depths of the dominant currents, the EUC and the SEC, at Jarvis during the 2000, 2001, and 2002 survey cruises. Current profiles taken ~4 km to the west of the island show EUC flow speeds strongest in 2000, with a strong eastward flow of 1.06 m s^{-1} centered at 145 m, and a broad profile spanning ~180 m of depth (Figure 4.1a). The westward SEC is also apparent in the profile, but is relatively weak (-0.10 m s^{-1}) in the upper 40 m. In 2001, currents near Jarvis show a weakening of the EUC and a strengthening of the SEC. The EUC core remains at a similar depth (140 m) as the previous year, but is nearly 0.20 m s^{-1} weaker with flow speeds peaking at 0.87 m s^{-1}. A stronger SEC (~0.25 m s^{-1}) is observed in 2001 with flows in the upper 40 m. In 2002, the EUC is weaker than in 2000, but similar to that of the previous year with flow speeds peaking at 0.83 m s^{-1}. Core depth deepens substantially to 180 m, which is ~40 m deeper than in 2000 and 2001. The SEC extends to a similar depth to that observed in 2001 but the flow speed weakens to 0.18 m s^{-1}.

SADCP profiles on the east side of the island differ substantially from those on the west (Figure 4.1b). In 2001, the SEC extends down to nearly 85 m with strong westward flow speeds near the surface (0.36 m s^{-1}). In 2002, the SEC is slightly shallower and weaker than in 2001. Westward flow comprises the upper 60 m with maximum flow speeds near the surface (~0.25 m s^{-1}). Below the SEC, the downstream profiles exhibit a weak and confused oscillatory flow pattern down to 250 m, likely associated with wake effects derived from island-EUC interactions.

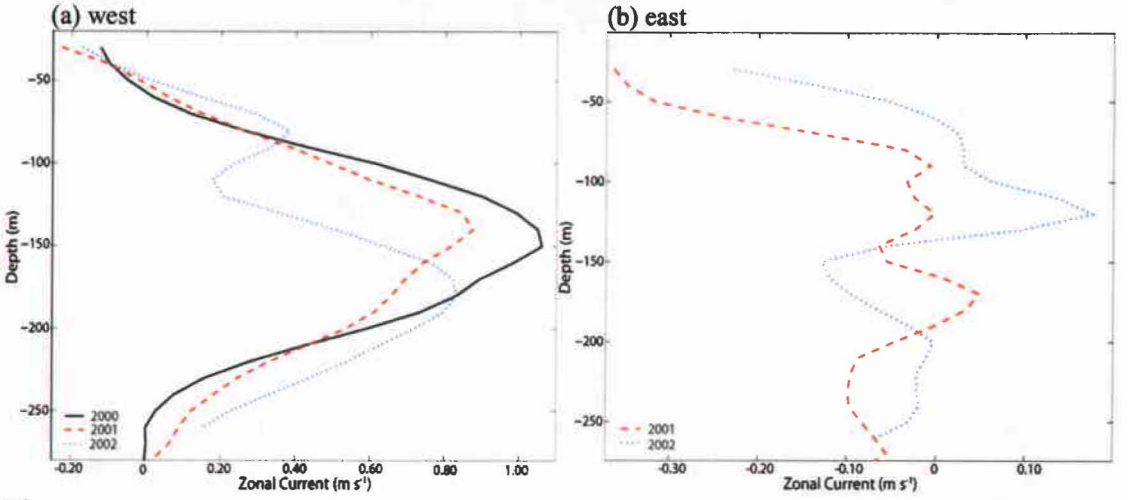

Figure 4.1. Zonal velocity as a function of depth measured ~4 km to the west (a) and east (b) of Jarvis Island during CRED survey years in 2000 (solid black line), 2001 (dashed red line) and 2002 (dotted blue line). Velocity was not measured to the east of Jarvis in 2000.

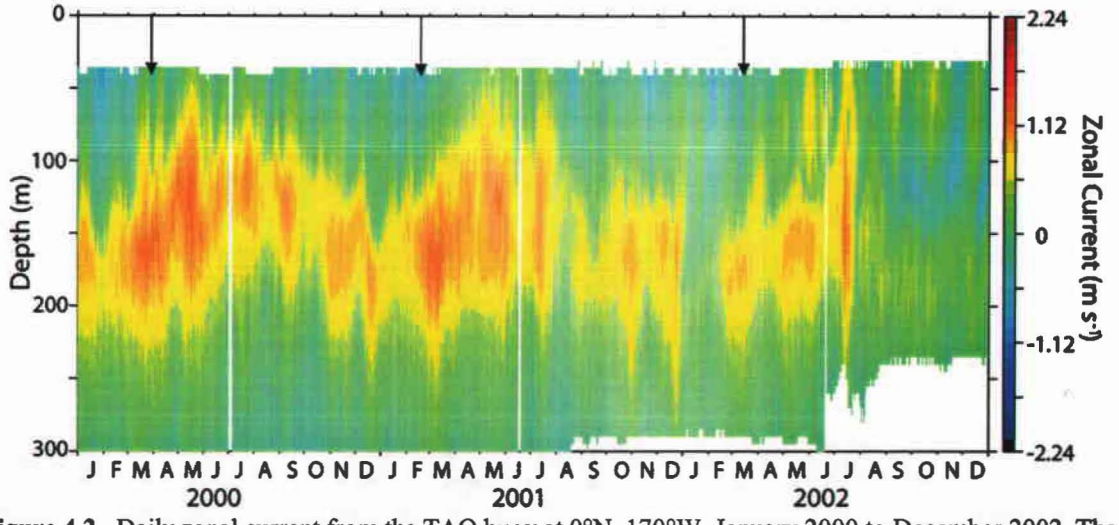

Figure 4.2. Daily zonal current from the TAO buoy at 0°N, 170°W, January 2000 to December 2002. The time period encompasses the CRED surveys of Jarvis Island indicated by the black arrows in March 2000, February 2001, and March 2002.

The depth and strength of the EUC measured at the TAO buoy at 0°N, 170°W are similar to the SADCP profiles on the upstream side of Jarvis (Figure 4.2). In all three hydrographic surveys, the EUC is 0.05 to 0.20 m s^{-1} faster at 170°W than that measured at Jarvis and 0 to 20 m deeper. The observed EUC depth difference is likely due the downward slope of the thermocline toward the west; the TAO buoy is ~1000 km to the

west of Jarvis. The decrease in flow speed at Jarvis relative to TAO is likely due to proximity (~4 km) of the SADCP observations to the island.

4.2 Sea Surface and Subsurface Temperatures

SST measured with the shipboard thermo-salinograph (TSG) around Jarvis shows evidence for upstream upwelling in each two-day CRED survey in 2000, 2001 and 2002 (Figure 4.3). SSTs are coldest just to the west of Jarvis, indicative of isotherms shoaling. In 2000, SST was ~25°C to the west of the island with surrounding waters between 0.5-1.5°C warmer (Figure 4.3a). In 2001, SSTs just west of Jarvis remain cold (25.3°C), however, the contrast with surrounding waters is less (0.7°C) than in 2000 (Figure 4.3b). In 2002, SST is significantly warmer (max 27.5°C) than in the two previous years; however, a pool of colder water (26.7°C) is still evident on the west side of Jarvis (Figure 4.3c).

The TSG data represent temporal as well as spatial variability, particularly associated with diurnal heating of surface waters. Although the residence time was not determined for upwelled waters, it is evident in Figure 4.3 that a variation of 0.5°C within 6-24 hours is not uncommon. In survey year 2000, for example, temperatures in a relatively confined area (~1.0 km^2) to the west of Jarvis show ~1.0°C change in < 24 hr period. We will show in Section 8 that changes on semidiurnal time scales may also be important for Jarvis SST.

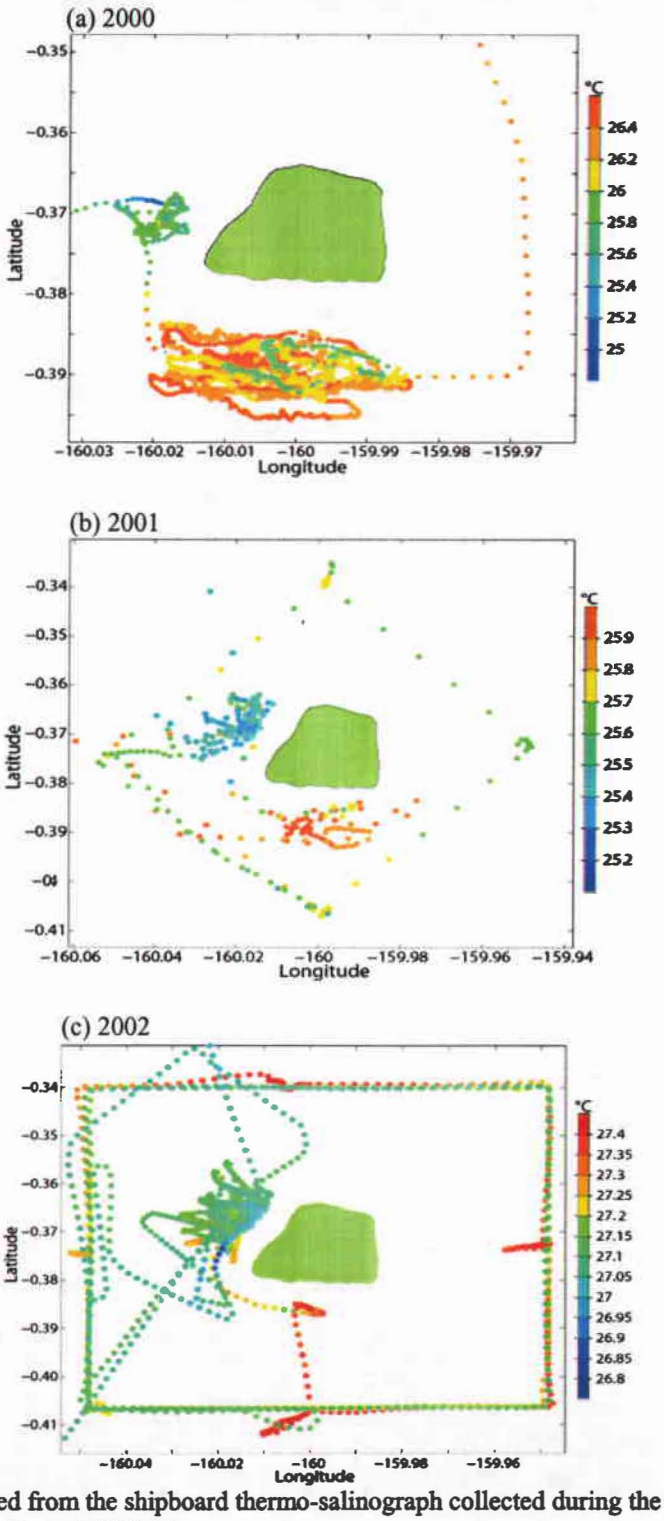

Figure 4.3. SST obtained from the shipboard thermo-salinograph collected during the CRED surveys at Jarvis in 2000 (a), 2001 (b), and 2002 (c).

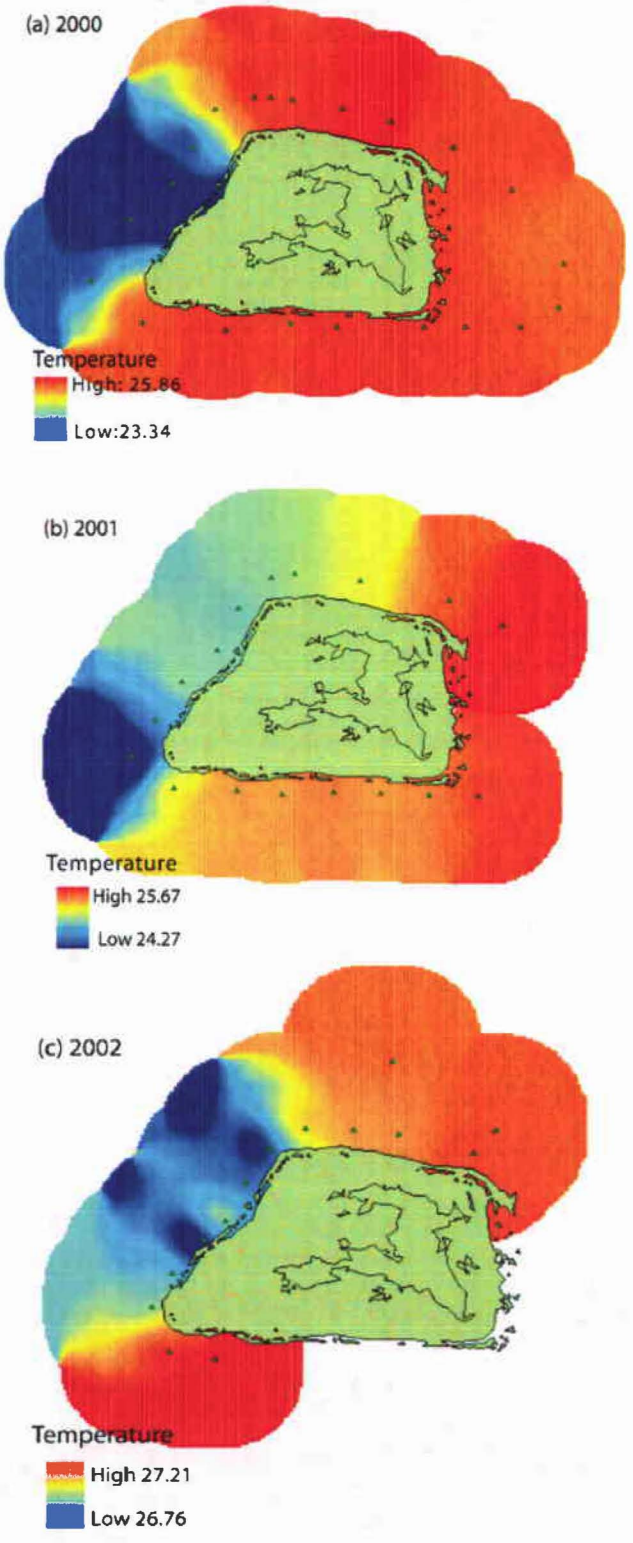

Figure 4.4. Temperature at 25 m derived from nearest neighbor interpolation of shallow water CTD casts at 25 meters for CRED survey years 2000 (a), 2001 (b), and 2002 (c).

Shallow water (30 m) CTD data (Figure 4.4) show that during all cruises the coldest near-surface temperatures occur on the west/southwest side of Jarvis Island, consistent with the SST. The coldest temperature at 25 m depth (23.34°C) and the largest contrast between temperatures on the western side compared to surrounding waters (2.52°C) occurred during the 2000 survey (Figure 4.4a). Outside of the cold pool, temperatures were nearly homogeneous at 25.86°C. In 2001, upwelling was strongest off the southwest tip of Jarvis, although the coldest measured temperature (24.27°C) is nearly a degree warmer than the coldest recorded in 2000 (Figure 4.4b). A 1.4°C difference is observed between the coldest (west side) and warmest (east side) recorded temperatures. The spatial distribution of upwelling is less defined compared to the previous year, with temperatures to the northwest showing intrusions of upwelled waters (note change in color scales in Figure 4.4). Of the three survey years, the weakest and most diffuse upwelling signal was observed during 2002 (Figure 4.4c). Equal-depth temperatures show a 0.46°C east-west difference. Upwelled waters were ~2.5°C warmer than the previous year.

The vertical structure of shallow water CTD profiles (Figure 4.5) varies considerably over the three surveys. In 2000, the water column was well mixed to a depth of 30 m in all casts except for the western most casts, which show variable stratification (Figure 4.5a). In the western upwelling profiles, a temperature difference of ~2.1°C occurs between the surface and 30 m depth. In 2001, vertical profiles show increased stratification from the previous year, with intrusions of cooler waters influencing multiple casts at 15-30 m depths (Figure 4.5b). Upwelling is most prevalent in the cast taken off the southwest tip of Jarvis, with surface temperature (25.49°C)

1.27°C warmer than at 30 m (24.22°C). Profiles taken in 2002 mostly show homogeneous upper layer temperatures (Figure 4.5c). Slight influences of cooler temperatures are observed near the lower 15-20 m with differences ranging from 0.3°C to 0.5°C.

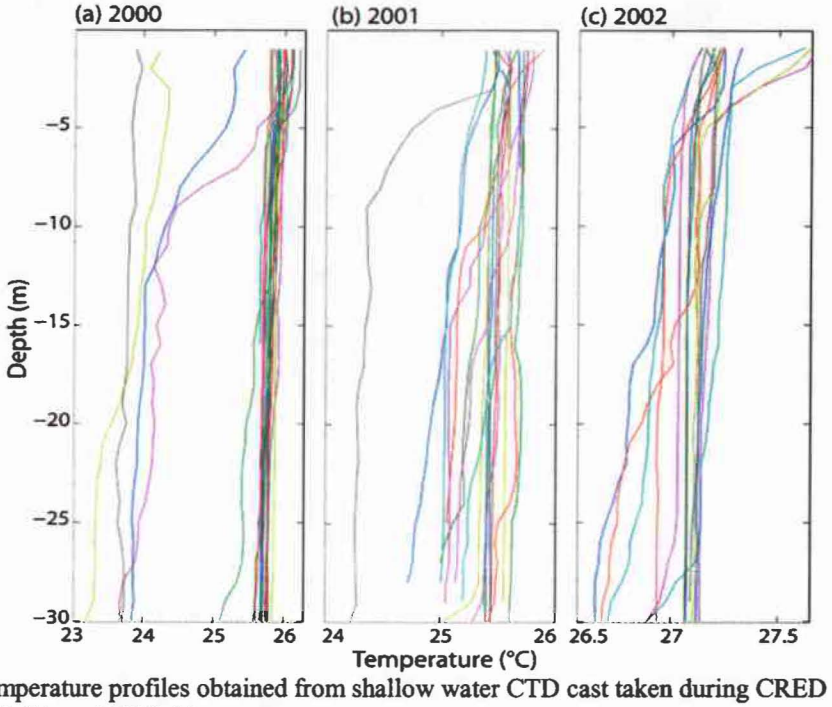

Figure 4.5. Temperature profiles obtained from shallow water CTD cast taken during CRED survey years in 2000 (a), 2001 (b), and 2002 (c).

As reported in R84, the 26°C isotherm generally marks the transition between the surface flow and the EUC. Here, we use the 25°C isotherm to represent the upper limit of EUC temperatures and to serve as a general indicator of variability and fluctuations in core depth. During the three surveys, the depth of the 25°C isotherm taken from TAO at 155°W (Figure 4.6) shows similar variations to those observed in the CRED hydrographic surveys at Jarvis. Isotherm depth is shallowest in the March 2000 survey, when 25°C temperatures shoaled to 13 m. In February 2001, the 25°C isotherm depth increased by over a factor of 3 to 55 m and in March 2002, the depth reached to 97

meters; a 42 m increase in depth from 2001 and an 84 m increase compared to 2000 observations.

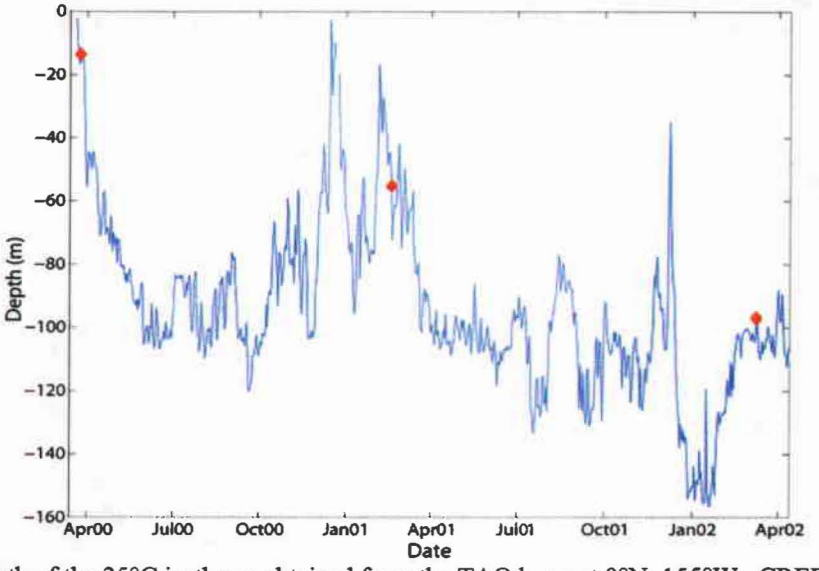

Figure 4.6. Depth of the 25°C isotherm obtained from the TAO buoy at 0°N, 155°W. CRED survey years (2000-2002) are shown as red diamonds.

4.4 Biological Data

Jarvis features a well-developed coral reef ecosystem (Maragos, 2004) however; the biological implications of variable upwelling are poorly understood. Upwelling of cool, nutrient rich water to reef ecosystems is potentially deleterious (Glynn et al., 1977; Atkinson and Falter, 2003) but episodic upwelling may influence the trophic structure and overall production of the ecosystem by serving as an important source of nutrients and suspended particles (Leichter and Miller, 1999).

Although various forcing mechanisms co-occur at Jarvis, upwelling is potentially influencing the zonation of the benthic community and favoring live coral growth (Figure 4.7). Analysis of towed diver benthic video taken in 2002 show live coral comprising over 50 percent of the benthic community to the west/southwest side of Jarvis, with

surrounding areas exhibiting predominantly algae and coral rubble and/or pavement substrate (Gove et al., unpublished data).

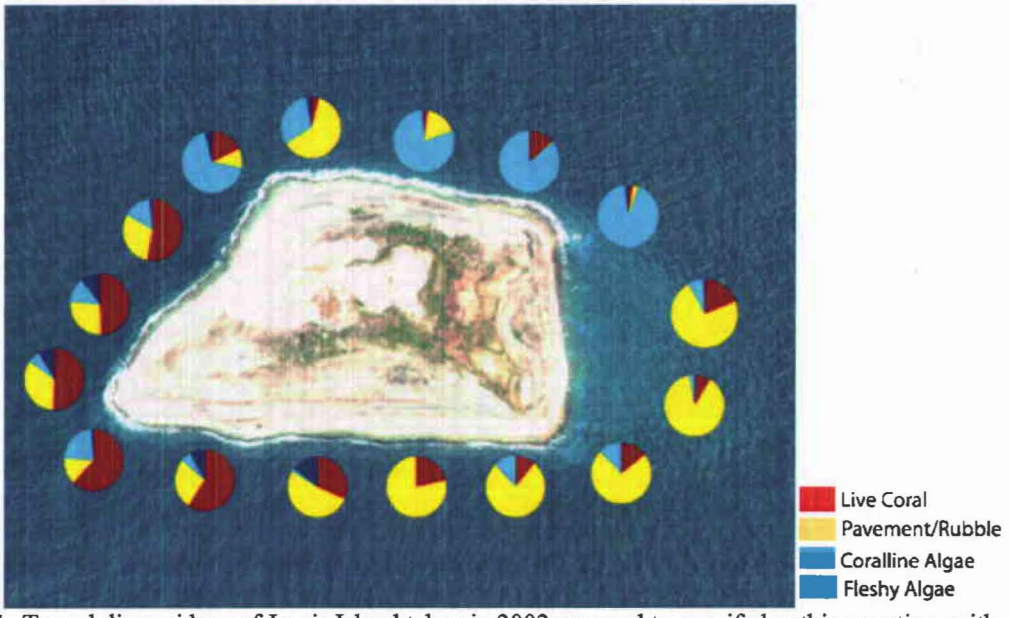

Figure 4.7. Towed diver videos of Jarvis Island taken in 2002 are used to specify benthic zonation, with live coral comprising a majority of the substrate to the west/southwest. Pie charts are 15 min averages and represent percentages of benthic substrate as indicated by the key to the right.

In addition, fish biomass distributions show influence of upwelling (Figure 4.8). Belt-transects at four locations around Jarvis show substantial differences in planktivore densities (mean range 8-137 fish 10 m^{-2}), with the greatest biomass densities occurring on the southwest tip of the island (Gove et al., unpublished data). No direct chlorophyll measurements were obtained; however, it is likely that the increase in nutrients associated with upwelling is stimulating planktonic growth, thereby increasing food availability and favoring greater planktivore densities.

Although the implications of variable upwelling to coral reef ecosystems have yet to be discerned, the injection of EUC waters and the presumed increase in nutrients is likely altering the trophic structure of the reef ecosystem near Jarvis Island.

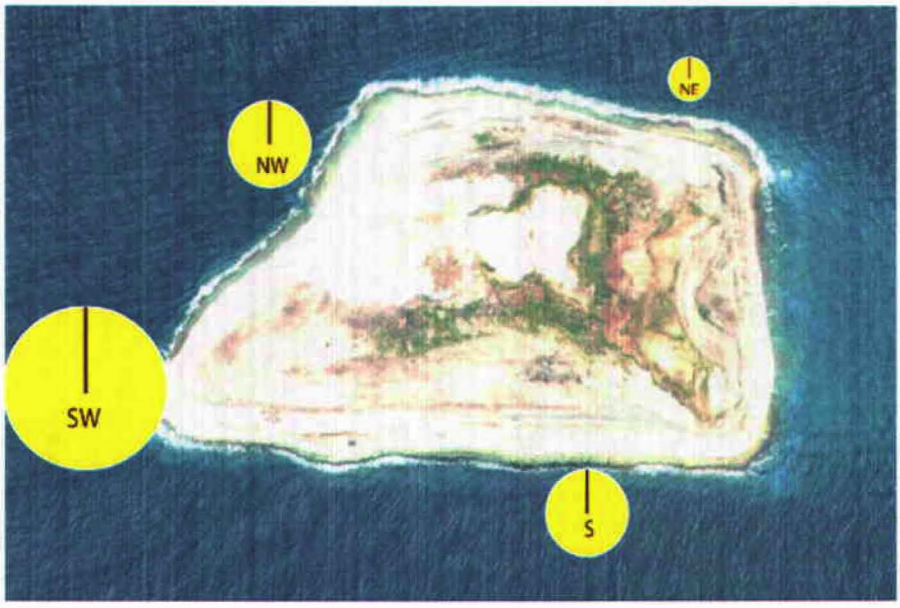

Figure 4.8. Stationary point counts at four survey sites around Jarvis performed in 2002 indicate increased planktivore densities on the southwest tip compared to surrounding areas. Densities have a mean range of 8-137 fish 10 m^{-2}

CHAPTER 5: TEMPORAL VARIABILITY OF UPWELLING

In-situ temperature measurements at 14 m water depth on the southwest tip of Jarvis from March 2002 to December 2003 provide the best available record of upwelling variability on the upstream side of the island. The time series shows low frequency variability, with changes of several degrees over weekly to monthly periods, superposed with sporadic episodes of high frequency fluctuations with amplitudes of 0.5 – 4.0°C (Figure 5.1a). Over the 22-month record, temperature ranged from 22.05 to 30.35°C with a mean of 27.85°C.

Upwelling occurs briefly in July 2002 but is mostly absent until boreal spring 2003 (Figure 5.1a). In April 2003, a distinct shift in near surface temperature occurs as variable upwelling dominates the record and temperatures are the coldest of the time series. Expanding this 3 month period, low frequency upwelling appears to be modulated on variable high frequency time scales (Figure 5.2). Sustained cooling from multiple days to weeks, rapid independent cold spikes, and semidiurnal fluctuations co-occur with low frequency upwelling. A power spectrum of the time series (Figure 5.3a) shows a well-defined semidiurnal tidal peak (period = 12.4 hr) along with a weaker peak at the harmonic (period ~ 6 hr).

Current data from the moored ADP is strongly oriented along local isobaths. Current is rotated into principal axes defined as 150° for positive alongshelf flow, and 60° for onshore flow. Only the dominant alongshelf component (150°/330°) is presented (Figure 5.1b). The data show episodic bursts of strong (peak of 1.30 m s^{-1}) positive alongshelf current lasting for 10-30 days, ephemeral pulses of weaker

(peak ~ -0.7 m s^{-1}) negative alongshelf flow, and sustained periods (e.g., January-April, 2003) when only weak tidal currents occur. Power spectrum for current shows energy peaking at the semidiurnal tidal frequency (Figure 5.3b). The dynamics of the alongshelf current bursts are discussed in Section 6.

Sea level at Christmas Island and the 25°C isotherm depth at 155°W compared with moored temperature and current at Jarvis illustrate the connection between large-scale forcing and near-shore variability (Figure 5.1c,d). Low frequency temperature changes (weeks to months) at Jarvis are related to changes in isotherm depth and sea level. The depth of the 25°C isotherm is the shallowest and sea level the lowest during boreal spring 2003 when upwelling at Jarvis is most prevalent. In addition, during the eastward (westward) current pulses at Jarvis, a contemporaneous increase (decrease) in sea level and deepening (shoaling) of the 25 °C isotherm occur (e.g., June-July 2002).

Zonal currents at TAO (170°W) vary seasonally as the EUC shoals and strengthens during boreal spring (the spring time surge, Keenlyside and Kleeman, 2002) and slackens and deepens in boreal fall and winter (Figure 5.1e). The EUC is substantially weaker in boreal spring to fall 2002 compared to the same time period in 2003 due to interannual variations. The current bursts observed at Jarvis also occur in near-surface currents in the TAO ADCP record; however, strong westward currents observed at TAO (January-April 2003) are not seen at Jarvis. We attribute this to the blocking of westward flows by the island, leaving only weak tidal flows on the western side.

Upwelling periods at the Jarvis mooring occur when isotherms are shallow, the EUC is shallow and strong, and sea level is low on a regional basis (Figure 5.1). This is

consistent with the EUC being the main forcing mechanism for island upwelling, with thermocline depth being a related (tied to EUC depth) and necessary condition. Upwelling therefore occurs seasonally (boreal spring) with obvious interannual modulations associated with ENSO variability (Figures 4.3-4.5, 5.1). It is also evident from Figure 5.1 that the strong eastward current bursts at Jarvis are not related to upwelling (e.g., June 2003). They are associated with surface current bursts at TAO with little expression in the EUC. In the next section, we relate upwelling and current burst variability to equatorial wind forcing, primarily in the western and central Pacific.

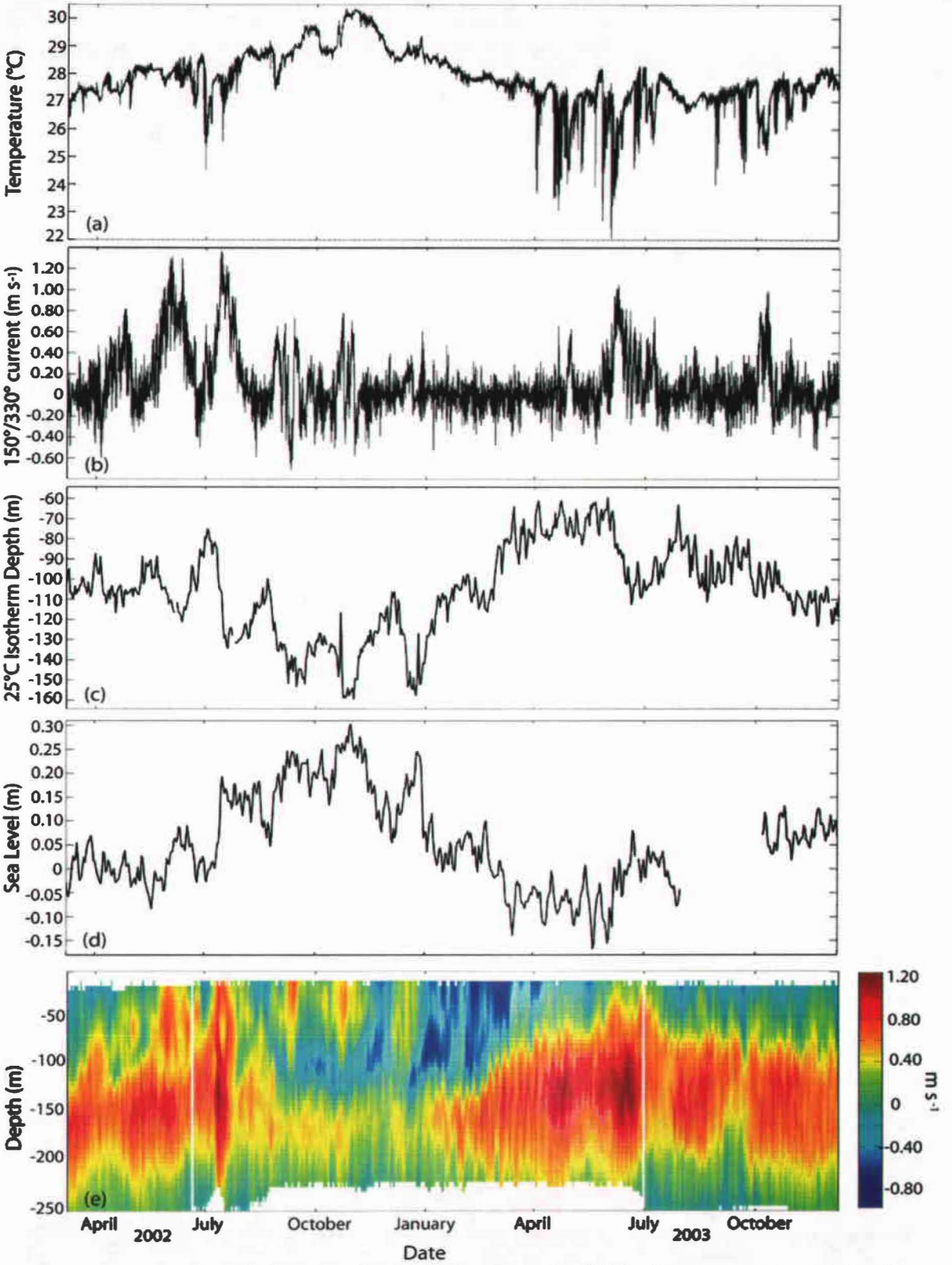

Figure 5.1. Twenty-two month time series (March 2002 to December 2003) of *in-situ* temperature (a) and alongshelf current (b) recorded at 14 m depth off the southwest tip of Jarvis, depth of the 25°C isotherm from TAO at 155°W (c), demeaned sea level from Christmas Island (d), and zonal currents from TAO at 170°W (e).

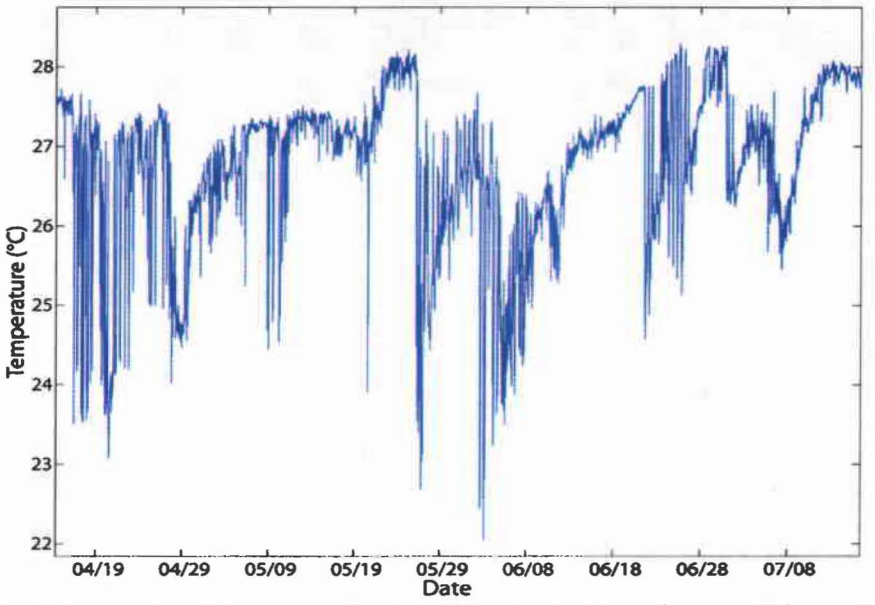

Figure 5.2. *In-situ* temperature (15 min sampling interval) taken in 14 m of water off the southwest tip of Jarvis from 15 April to 15 July 2003 show cold spikes occurring at ~12 hr periods.

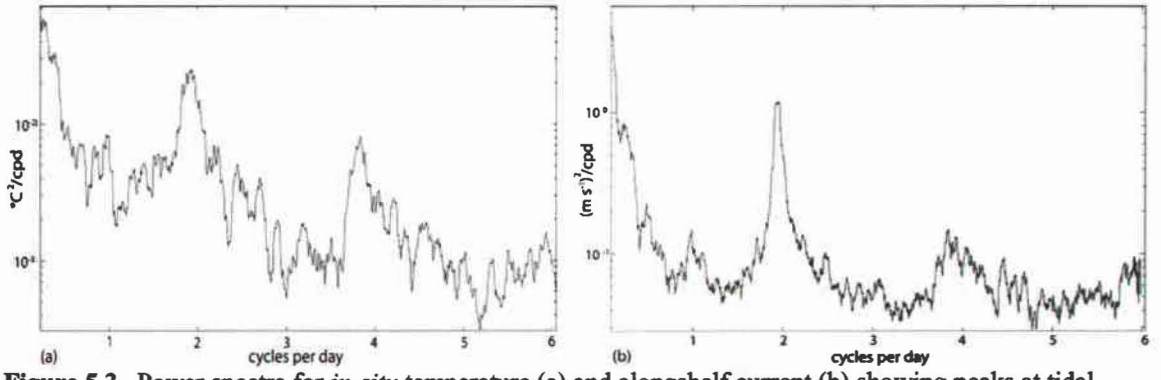

Figure 5.3. Power spectra for *in-situ* temperature (a) and alongshelf current (b) showing peaks at tidal frequencies.

CHAPTER 6: WIND VARIABILITY AND KELVIN WAVES

During the Jarvis mooring deployment (March 2002-December 2003), zonal wind conditions are characterized by steady trade winds with seasonal relaxations in the eastern Pacific, variable trades with occasional relaxation events in the central Pacific, and weak winds punctuated by westerly bursts in the western Pacific (Figure 6.1a). Westerly wind anomalies are prevalent in the western and central Pacific during boreal summer-fall 2002 (Figure 6.1b). Zonal wind variability is weak at Jarvis (160°W) compared to locations farther west.

As a result of fluctuating winds in the western Pacific, intraseasonal upwelling and downwelling Kelvin waves are generated (Miller et al., 1988; McPhaden et al., 1988; Kessler et al., 1995) producing variable sea level, thermocline depth and surface currents with eastward phase propagation (Enfield, 1987; McPhaden and Taft, 1988; Johnson and McPhaden, 1993) (Figure 6.1c,d). As expected, westerly wind bursts produce downwelling Kelvin waves with anomalously eastward surface currents (e.g., October 2002). Upwelling Kelvin waves with anomalous westward surface currents are observed following easterly winds in the western Pacific (e.g., December 2002), and in some cases following wind relaxation events (e.g., November 2002).

The strong eastward surface jets observed at Jarvis (Figure 5.1b) are predominantly related to regional wind forcing. The strongest eastward jets in boreal summer 2002 and 2003 are associated with a slackening of the trades across much of the basin (Figure 6.1a,b). Eastward jets result in response to a pressure gradient which is no longer in balance with the wind stress. At the TAO buoy (170°W) the eastward jets are most apparent in the upper 75 m of the water column (Figure 5.1e). Isotherm

displacements and sea level confirm that these current events are downwelling favorable (Figure 5.1c,d). As such, the EUC core tends to deepen during the eastward jets. In sum, these events are not favorable for upwelling at Jarvis.

The strong westerly winds in the western Pacific in boreal spring-fall 2002 cause the thermocline (here represented by the depth of the 20° isotherm) to deepen in the central to eastern Pacific, and shoal in the western Pacific (Figure 6.1e), in accordance with changes in the basin-wide zonal pressure gradient. This period coincides with seasonally high sea levels and deep isotherms in the central equatorial Pacific (Figure 5.1c,d). The main upwelling event at Jarvis in boreal spring 2003 is preceded by the slackening and/or weak reversal of the westerly winds in the western Pacific at the end of 2002. Anomalous upwelling (negative thermocline anomaly, Figure 6.1e) migrates eastward to Jarvis and the eastern Pacific in the form of an upwelling Kelvin wave. Therefore, remote winds and Kelvin wave propagation are instrumental for the main upwelling events observed during the Jarvis mooring deployment. Wyrtki and Eldin (1982) observed regional upwelling near Jarvis associated with local easterly wind anomalies. The upwelling periods observed in our Jarvis temperature record (Figure 5.1a) were not associated with easterly wind anomalies, although strong easterly wind events did not occur during our field measurements. To the extent that easterly winds cause a regional uplift of the EUC, we assume that EUC-driven upwelling at Jarvis would be enhanced by this mechanism.

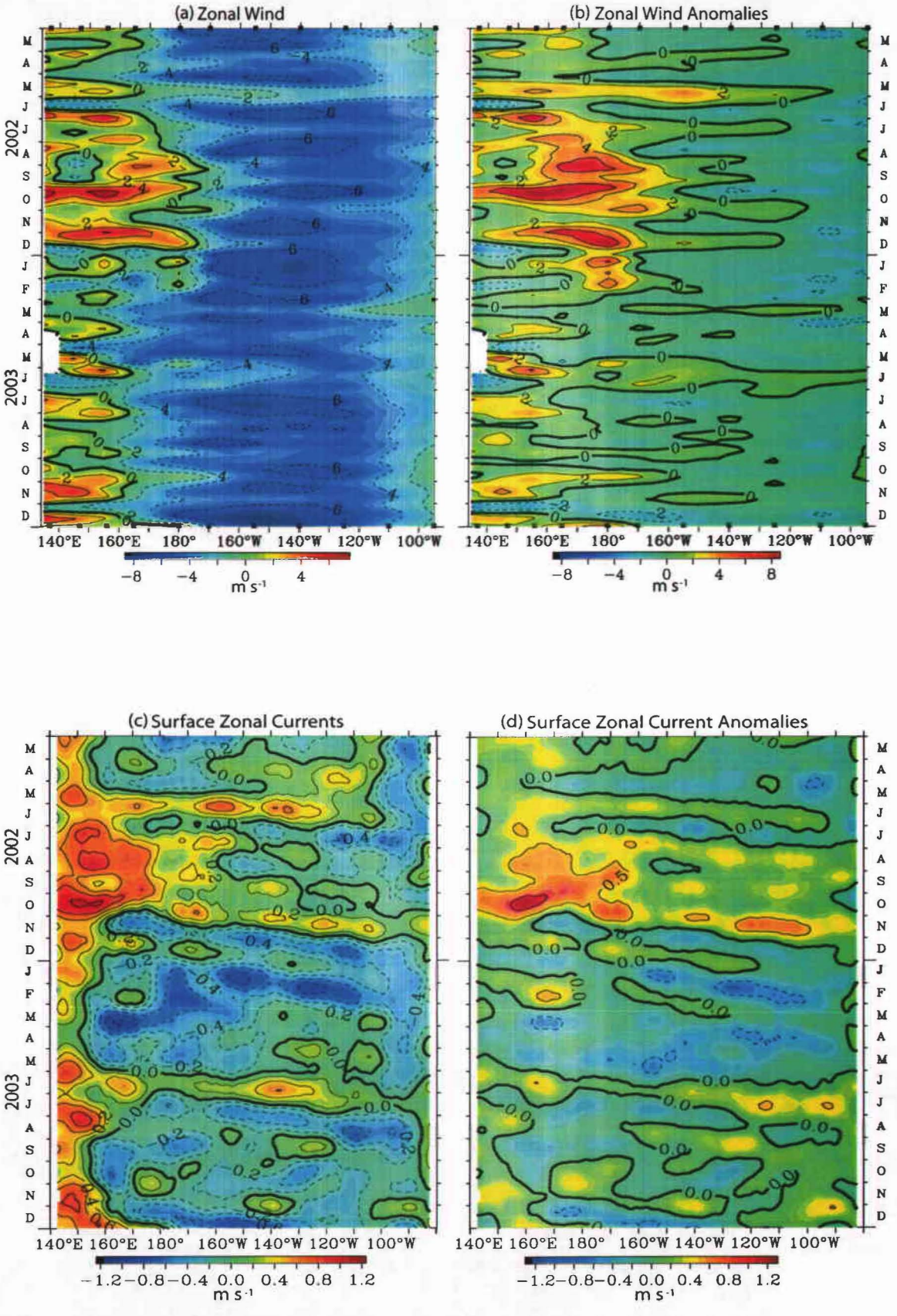
(a) Zonal Wind
(b) Zonal Wind Anomalies
(c) Surface Zonal Currents
(d) Surface Zonal Current Anomalies
2002
2003
M A M J J A S O N D J F M A M J J A S O N D
140°E 160°E 180° 160°W 140°W 120°W 100°W
−8 −4 0 4
−8 −4 0 4 8
−1.2 −0.8 −0.4 0.0 0.4 0.8 1.2
m s⁻¹

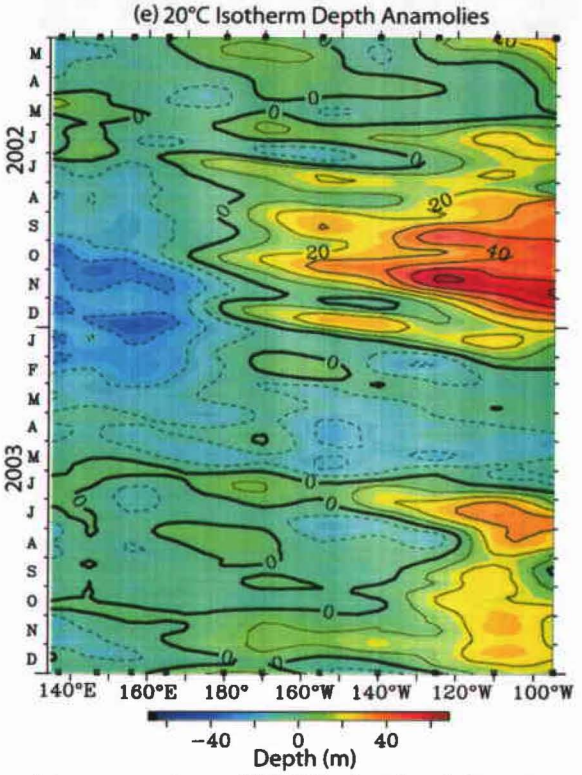

Figure 6.1. Longitude-time plots, averaged over 2°N-2°S, showing 5 day averaged zonal winds (a), zonal wind anomalies (b), estimated zonal surface current (c), estimated zonal surface current anomalies (d) and 20°C isotherm depth anomalies (e). All data are obtained from the TAO array, with the exception of estimated zonal surface currents which are derived from OSCAR.

The importance of equatorial Kelvin waves for establishing upwelling favorable conditions at Jarvis is illustrated further by examining the temperature anomaly versus depth across the Pacific before and during the 2003 boreal spring upwelling (Figure 6.2). The anomalous westerly winds west of 160°E cause warm sea surface temperature anomalies (SSTAs) in the central Pacific, warm subsurface temperature anomalies (STAs) in the central and eastern Pacific, and cool STAs west of the dateline (Figure 6.2a). The warm STAs indicate downward isotherm displacements which are most evident within the thermocline. Winds in the eastern Pacific are close to normal (zero anomaly), again emphasizing that the subsurface response in the eastern Pacific is set up by downwelling Kelvin waves originating in the west, and not by local wind forcing. The cold STAs in the western Pacific are consistent with a shallowing of the thermocline.

As the wind anomaly continues, the SSTA and STA strengthen (Figure 6.2b). In December 2002, following a brief cessation of winds, an easterly wind anomaly develops in the western Pacific, forcing an eastward propagation of the negative STA anomaly (Figure 6.2c). The negative STA in the eastern Pacific is due to a short wind relaxation in November, causing an upwelling wave to propagate to the east (Figure 6.1a,c,e). Through January to March 2003 winds across the Pacific relax to normal conditions, which coincides with a strengthening of cold STAs across the Pacific as the upwelling Kelvin wave propagates eastward (Figure 6.2d,e). In March, negative STAs are observed across the Pacific, indicating net equatorial upwelling of the thermocline for the entire basin (Figure 6.2e). Upwelling at Jarvis occurs during this period (Figure 6.2e,f).

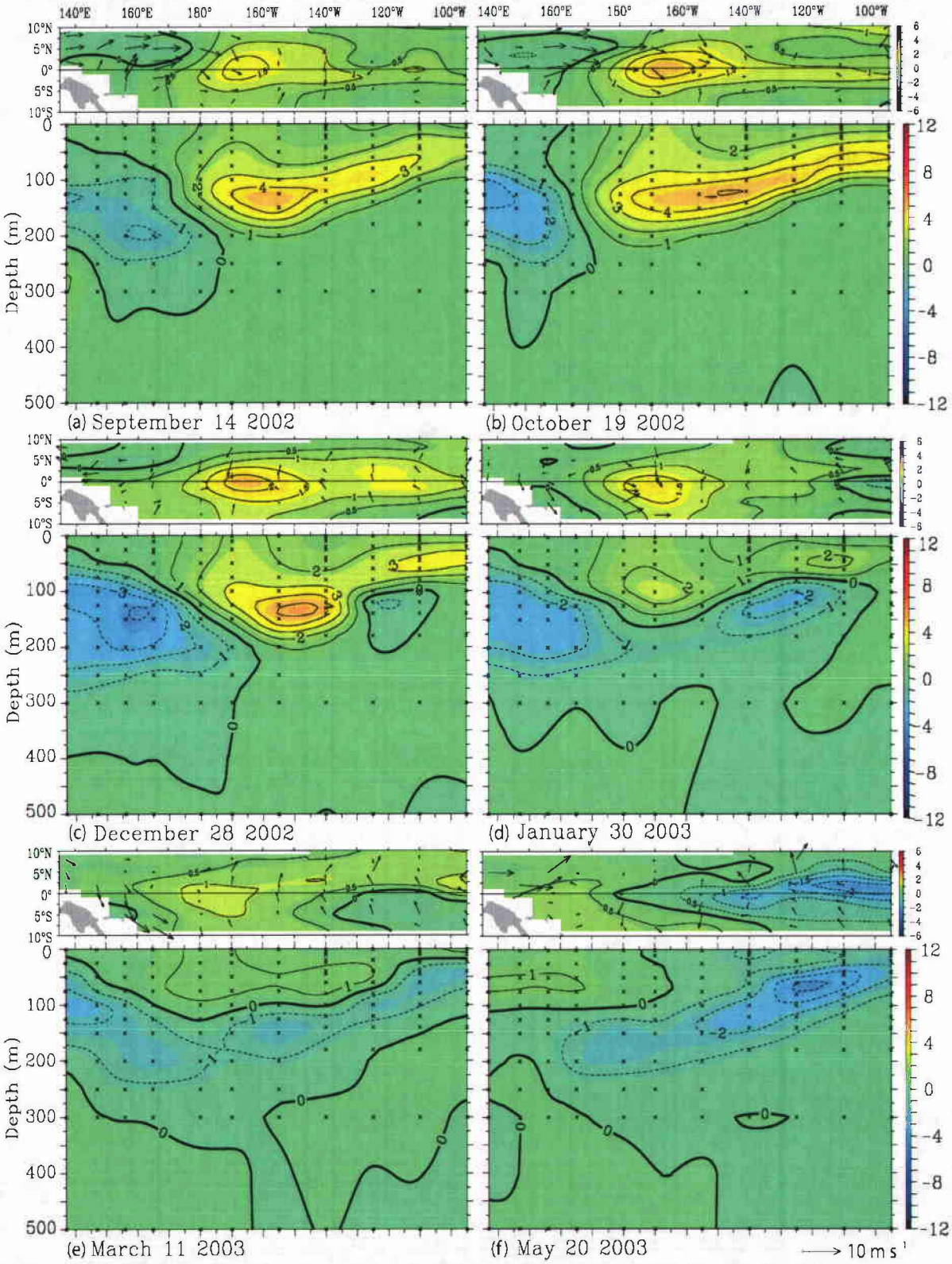

Figure 6.2. Five day averaged SST anomaly and wind anomaly vectors (top portion of each plot) and zonal temperature depth section anomalies averaged 2°N-2°S (bottom portion of each plot). Data are obtained from TAO, September 2002 to May 2003. Temperature anomalies are in °C and the wind anomaly scale is in the lower right corner.

CHAPTER 7: DIAGNOSTIC UPWELLING MODEL

Kelvin wave dynamics are important for determining the depth of the thermocline; however, it is the strength and depth of the EUC that is the main driving force for island-induced upwelling. To emphasize this point, we compare the observed upwelling at Jarvis with the theoretical model of HW73;

$$z - z_o = (U \frac{dU}{dz} \Big/ N^2)\Big|_{z=z_o}$$

We specify U and N from the surface to 250 m using ADCP and temperature data taken from TAO at 170°W to calculate theoretical isopycnal displacements for flow near Jarvis. Climatological salinity values are used to compute N. At each time step, we determine the deepest isotherm that upwells to the surface given the observed current and temperature structure. From this temperature we subtract the measured surface temperature at TAO to obtain the temperature difference (ΔT_M) caused by island-induced upwelling. We compare this with the observed upwelling at Jarvis (ΔT_{obs}), which is daily averaged SBE temperature minus an estimate of regional SST. Regional SST is obtained using the 9 km resolution Pathfinder SST which is interpolated to daily values. ΔT_{obs} is a measure of upwelling strength at Jarvis; subtracting regional SST ensures that upwelling events are specific to Jarvis and not a measure of regional wind-forced upwelling (e.g., Wyrtki and Eldin, 1982).

There is surprisingly good agreement between ΔT_M and ΔT_{obs} (Figure 7.1), particularly given the ~1000 km distance between the two sites. Upwelling periods (July 2002, April-July 2003, September-October 2003) are reproduced by the model, although the model tends to underestimate the observed upwelling, especially during peak events

(e.g., April-July 2003). The comparison presumably would improve with local measures of U, N and SST. The generally good agreement supports the conclusion that upwelling at Jarvis is a function of EUC strength and depth as well as thermocline depth.

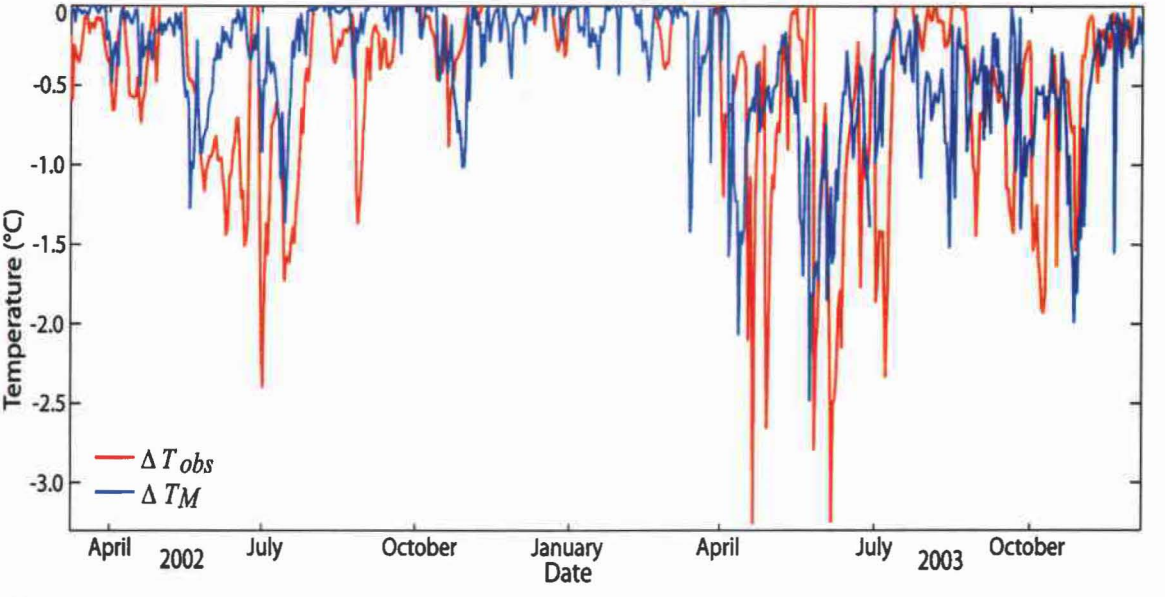

Figure 7.1. Dynamic upwelling model (ΔT_M) compared to observed upwelling (ΔT_{obs}) at Jarvis Island.

CHAPTER 8: UPWELLING AT TIDAL FREQUENCIES

During upwelling favorable conditions at Jarvis, abrupt cold spikes (1-4°C) tend to occur at ~12 hr periods (Figures 5.1-5.2, 8.1). In contrast, semidiurnal tidal currents occur more regularly throughout the entire time series. At the semidiurnal frequency, temperature and alongshelf currents are ~180° out of phase, such that maximum upwelling coincides with maximum eastward current. We do not have sufficient data to draw conclusions regarding the nature of the tidal upwelling. Multiple temperature sensors have been deployed around Jarvis that will help elucidate the high frequency signal. Until that data can be analyzed, we consider possible forcing mechanisms for the cold temperature spikes.

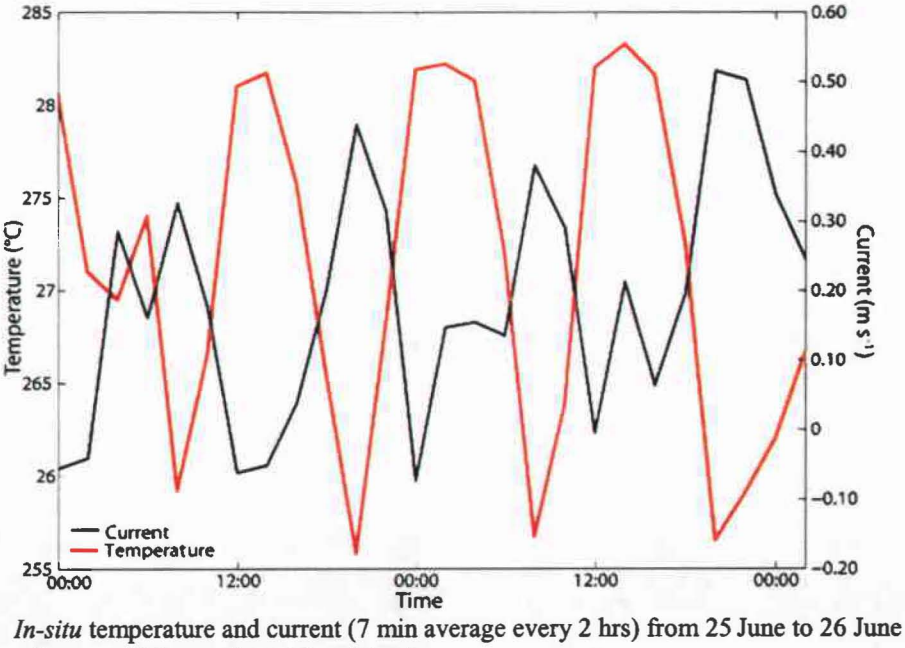

Figure 8.1. *In-situ* temperature and current (7 min average every 2 hrs) from 25 June to 26 June 2003 taken in 14 m of water off the southwest tip of Jarvis.

Barotropic tidal currents may cause horizontal advection of the cold upwelling patch located northwest of the mooring (Figure 4.4). Strong temperature gradients form off the southwest tip of Jarvis during times of upwelling. Barotropic tidal currents could potentially advect this gradient past the mooring at regular tidal intervals. Horizontal advection would result in cold temperature spikes lagging south-eastward current by 90°; however, observed currents and temperature are often 180° out of phase. It appears unlikely that horizontal advection alone can account for the observed temperature signal.

Barotropic tidal flow around Jarvis also may generate semidiurnal internal tides that enhance vertical isotherm displacements. This mechanism was cited to explain 100 m vertical displacements associated with the semidiurnal tide on the south shore of Oahu, Hawaii (Eich et al., 2004). Lacking a well-defined shelf region and given the steep slopes (supercritical relative to the semidiurnal internal tide) of the island, Jarvis is an unlikely location for strong internal tide generation (see Holloway and Merrifield, 1999 for a discussion of internal tide generation at isolated islands). Remotely generated internal tides that impinge on Jarvis might also play a role. Model simulations by Niwa and Hibiya (2001) show internal tide isotherm displacements up to 15 m in the region of Jarvis Island. This amount of additional isotherm displacement is consistent with the temperature tidal fluctuations observed at Jarvis during the main EUC-driven upwelling periods.

Cold temperature spikes at the semidiurnal frequency have been attributed to breaking internal waves, or internal tidal bores, that are generated at shoaling topography and propagate shoreward at regular tidal frequencies (Baines, 1986). Sharp drops in temperatures along the western coast of the U.S. (Piñeda, 1995), rapid temperature,

salinity, nutrient and current fluctuations at the near surface in the Florida Keys (Leichter et al., 1996, Leichter and Miller, 1999), and high frequency nutrient and temperature changes in Monterey Canyon (Shea and Broenkow, 1982) have been attributed to semidiurnal internal tidal bores. Again, given the steep island slopes, it is not clear how internal tidal bores might form at Jarvis. Detailed bathymetric surveys are needed to better assess tidal-topographic interactions.

CHAPTER 9: CONCLUSION

Variable upwelling on the western side of Jarvis Island has been linked to changes in the thermocline and the EUC, which are modulated by equatorial wind forcing on intraannual to interannual time-scales. While the importance of EUC-driven isotherm displacements at Jarvis has been known since the 1970s, we have tried to emphasize the temporal variability of near-surface temperatures and how it is linked to well-studied aspects of wind-forced equatorial dynamics. Wind variability in the equatorial Pacific affects the depth of the EUC, and hence upwelling at Jarvis on a variety of time scales. At seasonal time scales, island-induced upwelling tends to occur in boreal spring owing to wind relaxations in the eastern Pacific (Keenlyside and Kleeman, 2002). At intraannual and interannual time scales, wind fluctuations in the western Pacific are more important for determining upwelling at Jarvis. In general, La Niña conditions favor upwelling at Jarvis by inducing a regional shoaling of the thermocline and the EUC.

Based on long term sea level measurements, a proxy for thermocline depth (Rebert et al, 1985), we can now put the previous survey observations at Jarvis into a similar context. Five of the six observation periods have occurred during times of low to average sea level height, or equivalently, during mild upwelling conditions (Figure 9.1). Only the November 1982 observations described by R84 occurred during a strong El Niño phase, when the EUC was anomalously weak in the central Pacific. Interestingly, observations have not been obtained during maximum La Niña phases; the strongest upwelling at Jarvis has yet to be sampled.

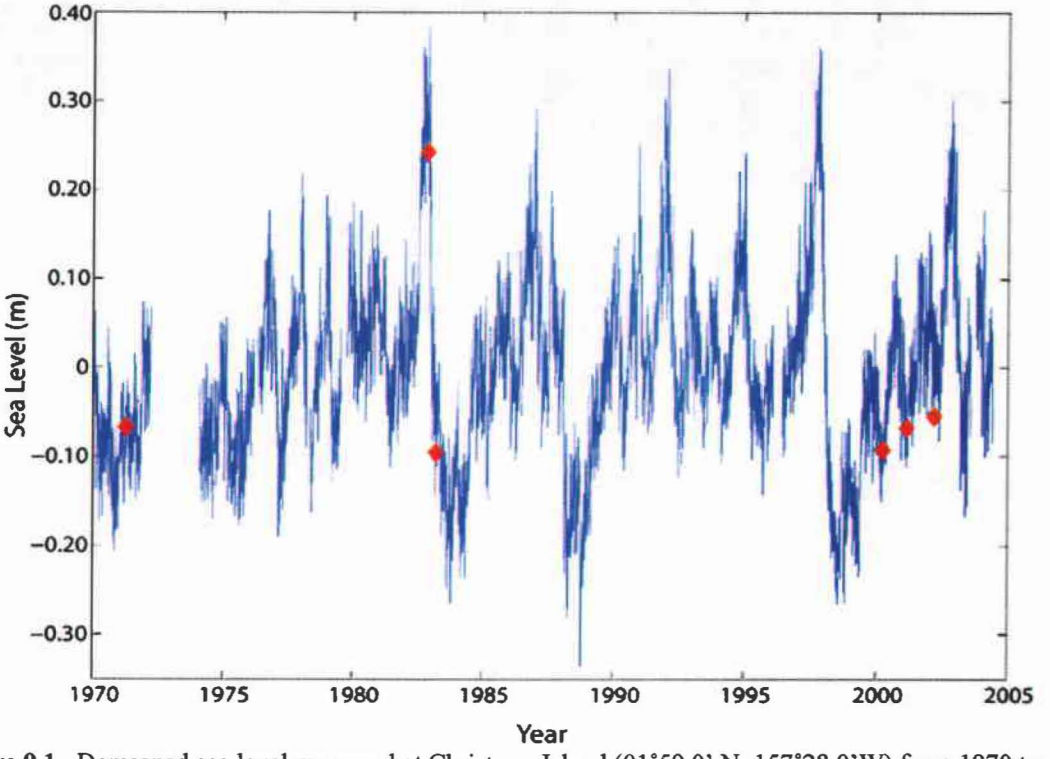

Figure 9.1. Demeaned sea level measured at Christmas Island (01°59.0' N, 157°28.0'W) from 1970 to 2005. Red diamonds represent surveys performed at Jarvis by CRED (2000, 2001, 2002), Roemmich (1984) (November 1983; March 1984), and Hendry and Wunsch (1971).

Moored temperature observations provide the first indication of tidally-driven upwelling at Jarvis. Similar tidal upwelling spikes have been observed at a Florida reef (Leichter et al, 1996, Leichter and Miller, 1999). During EUC-driven upwelling, the tide can cause abrupt temperature drops of 1-4°C every 12 hours. Given the available evidence, we believe that internal tides, either locally or perhaps remotely generated, are the most likely mechanism for the temperature variations.

Localized upwelling on the western side of Jarvis shows a marked influence on the coral reef ecosystem. Benthic habitat surveys show live coral comprising > 50 percent of the benthic community to the west/southwest side of Jarvis with surrounding waters having significantly less, consistent with the upwelling pattern. Likewise, planktivore densities are an order of magnitude greater off the southwest of the island compared to surrounding locations. Although the biological implications of variable

upwelling have yet to be determined, the injection of EUC waters and the presumed increase in nutrients appears to be altering the reef community near Jarvis Island. Future studies are needed to examine the ecological importance of variable upwelling on the spatial and temporal dynamics of the reef ecosystem.

REFERENCES

Atkinson, M., and Falter, J., 2003: Coral Reefs. *In* Biogeochemistry of Marine Systems. *CRC Press*, 40-64.

Baines, P. G., 1986: Internal tides, internal waves, and near inertial motions. *Baroclinic processes on continental shelves.* **3,** 19-31.

Chavez, F., Strutton, P., Friederich, G., Feely, R., Feldman, G., Foley, D., McPhaden, M., 1999: Biological and chemical response of the equatorial Pacific Ocean to the 1997-1998 El Niño. *Science.* **286,** 2126-2131.

Christensen, N., 1971: Observations of the Cromwell Current near the Galapagos Islands. *Deep-Sea Research.* **18,** 27-33

Cromwell, T., 1953: Circulation in a meridional plane in the central equatorial Pacific. *Journal of Marine Research.* **12,** 196-213.

Drazin, P., 1961: On the steady flow of a fluid of variable density past an obstacle. *Tellus.* **13,** 239-251.

Eich, M., Merrifield, M., and Alford, M., 2004: Structure and variability of semidiurnal internal tides in Mamala Bay, Hawaii. *Journal of Geophysical Research.* **109** (C05010).

Enfield, B., 1987: The intraseasonal oscillation in eastern Pacific sea levels: How is it forced? *Journal of Physical Oceanography.* **17,** 1860-1876.

Firing, E., 1981: Current profiling in the NORPAX Tahiti Shuttle. *Tropical Ocean-Atmosphere Newsletter.* **5.**

Firing, E., Lukas, R., Sadler, J., Wyrtki, K., 1983: Equatorial Undercurrent disappears during 1982-1983 El Niño. *Science.* **222,** 1121-1123.

Foley, D., Dickey, T., Mcphaden, M., Bidigare, R., Lewis, M., Barber, R., Lindley, S., Garside., Manov, D., Mcneil, J., 1997: Longwaves and primary productivity variations in the equatorial Pacific at 0°, 140°W. *Deep-Sea Research II.* **44,** (9-10), 1801-1826.

Glenn, P., 1977: Coral growth in upwelling and non-upwelling areas off the Pacific coast of Panama. *Journal of Marine Research.* **35,** 567-585.

Gove, J., Dunlap, M., and Schroeder, R.: Unpublished.

Hendry, R., and Wunsch, C., 1973: High Reynolds number flow past an equatorial island. *Journal of Fluid Mechanics*. **58,** (1) 97-114.

Holloway, P., and Merrifield, M., 1999: Internal tide generation by seamounts, ridges, and islands. *Journal of Geophysical Research.* **104,** 25937-25951.

Johnson, E., and McPhaden, M., 1993: On the structure of intraseasonal Kelvin waves in the equatorial Pacific Ocean. *Journal of Physical Oceanography*. **23,** 608-625.

Keesler, W., McPhaden, M., and Weickmann, K., 1995: Forcing of intraseasonal Kelvin waves in the equatorial Pacific. *Journal of Geophysical Research*. **100,** (C6), 10613-10632.

Keenlyside, N., and Kleeman, R., 2002: Annual cycle of equatorial zonal currents in the Pacific. *Journal of Geophysical Research*. **107,** (C8), 1-13.

Kenyon, J., Brainard, R., Hoeke, R., Parrish, F., Wilkinson C., 2004: Towed-diver surveys, a method for mesoscale spatial assessment of benthic reef habitat: a case study at Midway Atoll in the Hawaiian Archipelago. *Proc. Coastal Zone Asia-Pacific Conference*, Brisbane, Australia

Knauss, J., 1960: Measurements of the Cromwell Current. *Deep-Sea Research.* **6,** 265-285.

Koop, K., Booth, D., Broadbent, A., Brodie, J., Bucher, D., Capone, D., Coll, J., Dennison, W., Erdmann, M., Harrison, P., Hoegh-Guldberg., Hutchings, P., Jones, G., Larkum, A., O'neil, J., Steven, A., Tentori, E., Ward, S., Williamson, J., and Yellowless, D., 2001: ENCORE: The effect of nutrient enrichment on coral reefs. Synthesis of results and conclusions. *Marine Pollution Bulletin.* **45** (2), 91-120.

Lamb, H., 1932: Hydrodynamics. *Cambridge University Press*.

Leichter, J., Wing, S., Miller, S., Denny, M., 1996: Pulsed delivery of subthermocline water to Conch Reef (Florida Keys) by internal tidal bores. *Limnology and Oceanography*. **41,** (7), 1490-1501.

Leichter, J., and Miller, S., 1999: Predicting high-frequency upwelling: Spatial and temporal patterns of temperature anomalies on a Florida coral reef. *Continental Shelf Research*. **19,** 911-928

Mann, K., and Lazier J.R.N., 1996: Dynamics of Marine Ecosystems: Biological-physical interactions in the Oceans. *Blackwell*, Cambridge, MA.

Maragos, J., 2004: Monitoring corals and other macro-invertebrates at fixed sites at US Pacific remote and atolls. *10th International Coral Reef Symposium – abstracts.* 137.

McPhaden, M., 1999: Genesis and evolution of the 1997-1998 El Niño. *Science.* **283,** 950-953.

McPhaden, M., Busalacchi, A., Cheney, R., Donguy, J., Gage, K., Halpern, D., Ji, M., Julian, P., Meyers, G., Mitchum, G., Niiler, P., Picaut, J., Reynolds, R., Smith, N., and Takeuchi, K., 1998: The Tropical Ocean-Global Atmosphere observing system: A decade of progress. *Journal of Geophysical Research.* **103,** (C7), 14-169, 240.

McPhaden, M., Freitag, H., Hayes, S., Taft, B., Chen, Z., and Wyrtki, K., 1988: The response of the equatorial Pacific Ocean to a westerly wind burst in May 1986. *Journal of Geophysical Research.* **93,** (10), 589-10, 603.

McPhaden, M and Taft, B., 1988: On the dynamics of seasonal and intraseasonal variability in the eastern equatorial Pacific. *Journal of Physical Oceanography.* **18,** 1713-1732.

Miller, L., Cheney, R., and Douglas, B., 1988: Geosat altimetry observations of Kelvin waves and the 1986-1987 El Niño. *Science.* **239,** 53-54.

Niwa, Y., and Hibiya, T., 2001: Numerical study of the spatial distribution of the M_2 internal tide in the Pacific Ocean. *Journal of Geophysical Research.* **106,** (C10), 22441-22450.

Noble, M., and Xu, J., 2003: Observation of large-amplitude cross-shore internal bores near the shelf break, Santa Monica Bay, CA. *Marine Environmental Research.* **56,** 127-149.

Pak, H., and Zaneveld, J., 1973: The Cromwell Current on the east side of the Galapagos Islands. *Journal of Geophysical Research.* **78,** (33), 7845-7859.

Philander, S., 1990: El Niño, La Niña and the Southern Oscillation. *Academic Press.*

Pineda, J., 1995: An internal tidal bore regime at near shore stations along western U.S.A.: Predictable upwelling with the lunar cycle. *Continental Shelf Research,.* **15,** 1023-1041

Rebert, J., Donguy, J., Eldin, G., and Wyrtki, K., 1985: Relationships between sea level, thermocline depth, heat content and dynamic height in the tropical Pacific Ocean,. *Journal of Geophysical Research.* **90,** (11), 719-11, 725.

Roemmich, D., 1984: Indirect sensing of equatorial Currents by means of island pressure measurements. *Journal of Physical Oceanography*. **14,** (9) 1458-1469.

Schroeder, R., Trianni, M., Moots, K., Zgliczynski, B., Laughlin, J., Tibbetts, B., and Capone, M., 2004: Status of fishery target species on coral reefs of the Marianas Archipelago. *10th International Coral Reef Symposium – abstracts.*

Szmant, A.M., 2002: Nutrient enrichment on coral reefs: is it a major cause of coral reef decline? *Estuaries*. **25,** (4b), 743-766.

Yu, X., and McPhaden, M., 1999: Seasonal Variability in the Equatorial Pacific. *Journal of Physical Oceanography*. **29**, 925-947.

Wyrtki, K., and Eldin, G., 1982: Equatorial upwelling events in the central Pacific. *Journal of Physical Oceanography*. **12,** 984-988.

Wyrtki, K., and Kilonsky B., 1984: Mean Water and Current Structure during the Hawaii-to-Tahiti Shuttle Experiment. *Journal of Physical Oceanography.* **14,** 242-254.

Wyrtki, K., E. Firing, D. Halpern, R. Knox, G.J. McNally, W.C. Patzert, E.D. Stroup, B.A. Taft, and R. Williams. 1981: The Hawaii to Tahiti shuttle experiment. *Science.* Vol. 211(4477) 22–8